MAGNETOHYDRODYNAMICS Vol. 41 (2005), No. 2, pp. 199–211

Characteristics of velocity pulsations in turbulent recirculated melt flow

M. Kirpo[1], *A. Jakovičs*[1], *E. Baake*[2]

[1] *Laboratory for mathematical modeling of environmental and technological processes, University of Latvia, Zeļļu 8, Rīga, LV-1002, Latvia*

[2] *Institut für Elektrothermische Prozesstechnik, Universität Hannover, Wilhelm-Busch-Str. 4, 30167 Hannover, Germany*

For the modern industrial applications it is necessary to develop and investigate metallic and oxide materials of a high purity or predicted composition. Such materials can be produced by the induction melting method, especially in inductor and cold crucible furnaces. Measurements taken in experimental furnaces show that the velocity pulsations are dominated for the heat and mass exchange in melt, especially in a zone between typical upper and lower eddies. Understanding of pulsations mechanism and development of models for estimation of exchange characteristics are very important for development and optimisation of industrial furnaces. The authors present experimental results and propose a simple 3D large eddy simulation (LES) model of induction furnace that can be adapted for qualitative analysis of experimental data.

Introduction The modern industry and technology always look for new materials with definite physical properties: low weight, high mechanical durability and high working temperature; it is also required that they be cheaply produced, possessing at the same time high quality. The induction melting is one of the best known technologies that can be used for production of metals, oxides and glasses. In this technology electromagnetic field generates currents and Joule heat in a material, forms a free surface and influences the flow of melt. The melt flow formed by the Lorentz forces is often turbulent and has a complex structure. To improve electromagnetic furnaces it is necessary to achieve technologically defined superheat of the melt that is needed for doping and casting [1] with the lowest energy consumption.

Characteristics of the melt flow in such processes are very important because they determine heat-and-mass transfer in the melt. There are known experimental data on Wood's alloy flows in conventional crucible [2], which can be computer simulated. Experimental data of the kind can be compared only with the results of computer modeling, since turbulent fluid flows, which are widespread in the nature and technologies, present one of the problems that mostly cannot be solved analytically. Wellknown and fast semi-empirical computer models used in engineering calculations often give results that differ from experimental [3]. Empirical constants of such models should be corrected or more complicated 3D models (DNS, LES) of the flow should be used to obtain more precise calculation results.

1. Experimental In the experiments, electromagnetically driven flow of Wood's metal was studied [2]. Wood's metal was placed in a steel crucible, 0.57 m high and 0.316 m in diameter, to which electromagnetic field with a frequency ranged from 300 to 1500 Hz was applied (figure 1). The current of a 10-coil inductor 1000 A to 2200 A. The crucible was water-cooled. In the experiment, a

constant melt temperature of about 80^oC was achieved. The radial and axial components of the melt flow velocity were measured by a permanent magnet sensor (scanning rate from 20 to 100 Hz) for 60 second in every point of discrete grid. Filling level of the melt was varied from 50 to 120% of the inductor height, but in most of the experiments the filling level was equal to the inductor height (100%). Analysis of experimental data shows that the average flow consists of two dominating toroidal vortices (figure 2). The momentum, heat and mass are mainly transferred from one vortex to the other with low-frequency and turbulent flow velocity oscillations, which are observed in the turbulent flow between the main vortices in the middle zone of the melt [2]. Each velocity component oscillates, but the intensity and spectral energy distribution of the oscillations depend on the place; for example, radial velocity oscillations between the eddies near a wall are slightly reduced by the crucible walls (figure 3). The oscillations have some structure and their basic frequency can be found. The turbulence is the most expressed in the zone between the eddies too. The whole flow can conditionally be divided into three parts $\vec{v} = \vec{v_m} + \vec{v_l} + \vec{v_t}$ depending on its behavior:

1. the average flow, $\vec{v_m}$, which forms the main toroidal vortices with velocities averaged in time;
2. the low frequency velocity oscillations, $\vec{v_l}$, which are defined by the interaction of vortices and the development of coherent structures;
3. the turbulent flow, $\vec{v_t}$, which mainly depends on the local characteristics of the flow with energy dissipation by small-scale velocity oscillations.

2. Experimental results and discussion Special software was developed for analysing the experimental data. First, some well-known dependences were verified to make sure that measured velocity values correspond to the previous theoretical conclusions. Figure 4 shows the maximum axial velocity v_{zmax} depending on the inductor current I for different EM field frequencies at the symmetry axis point r=0, z=130 mm. This means that all experimental series can be approximated with lines. The angle between the approximation line and the current axis depends on the inductor frequency F, but to a less degree: $v_{ch} \sim \frac{1}{\sqrt{F}}$ [2]. Therefore this angle changes slightly in the working frequency region, so it can be suggested that characteristic velocities are almost frequency-independent within the accuracy of experimental data.
In the experiments the flow intensity varied from 4 to 22 cm/s and the Reynolds number $Re = \rho\frac{v \cdot r}{\mu}$, where ρ is melt density (ρ=9400 kg/m^3), r is characteristic distance, μ is dynamic viscosity (μ=4.2·10^{-3} $\frac{N \cdot s}{m^2}$), was greater then 10^4 in experiments, hence the flow is highly turbulent. In industrial facilities the Reynolds values can even be 10÷100 times greater.
The analyzed turbulent flow is higly anisotropic. The turbulence is more or less isotropic only in the central zones of the vortices (figure 7). The changes in axial velocity are two-three times greater than the radial velocity oscillations $|v'_z|/|v'_r|_{max} \approx 2.5$ near the wall (figure 9), where radial pulsations are cut down by the wall effect. The axial velocity has very expressive oscillations there, which are influenced by two melt jets going near the crucible wall in opposite directions. The radial velocity pulsations are dominating in the central region between the vortices (figures 6, 8): $|v'_z|/|v'_r|_{max} \approx 0.6$. The wall effects at the crucible center are negligible and the flow there is mainly determined by inertia, while the unbalance of radial and axial velocity pulsations is smaller. The radial velocity

oscillations are greater, since two horizontal flow jets, going in opposite directions form a flow in this zone.
The maximum energy of pulsations between the vortices can be 10 times greater than characteristic pulsation energy in other regions near the wall (figure 5). This difference is smaller when both vortices are more or less equal (filling level is about 90÷100%). The energy level of pulsations increases when the intensity of the vortices has a larger unbalance (filling level is less than 70% or greater than 120%). The basic energy level at the top and at the bottom of the crucible is almost equal for any filling, because this energy is defined by usual small-scale turbulence. In the zone between eddies the kinetic energy is much greater because the macroeffects of low-frequency oscillations are more expressed there.
Comparison of the experimental data with the results of 2D isotropic turbulence models shows that two-parameter models do not allow correct results to be obtained about the heat-and-mass transfer between such eddies, because the energy maxima are in the vortex centers, whereas the experiments show that the maximum pulsation energy is in the zone between eddies, where the convective transfer of the averaged flow is close to zero [3]. Therefore macroscopic pulsations significantly influence transfer processes. The empirical approach in engineering models when the value of turbulent Prandtl number $\mathrm{Pr}_t = \frac{\upsilon_t}{\lambda_t}$, where υ_t is kinematical turbulent viscosity and λ_t is turbulent thermal diffusivity, is artificially decreased to 0.01, leads to increased heat transfer in the whole melt. Moreover, the turbulent viscosity achieves its maximum value near the center of averaged vortex in a traditionally used $k - \varepsilon$ model, but it is relatively low in the vortex interaction zone. Hence the artificial decrease in the Prandtl number leads to incorrect heat-and-mass transfer modelling results.

I, A	F, Hz	Eddy period, s	Pulsation period, s	$\langle v \rangle$, cm/s
1068	1444	12.6	13	5.50
1260	1470	10.5	15	6.62
1670	990	6.4	8	10.84

Table 1: Characteristic velocities and periods of the flow and velocity pulsations

The characteristic values of pulsation periods and vortex circulation periods for different inductor currents and the characteristic points of flow are shown in table 1. The values of pulsation periods are of the same order as those of the circulation periods. The eddy circulation period was calculated using a simple formula:

$$L = 2\pi \cdot \left(\frac{r_r + r_z}{2}\right); \quad T = \frac{L}{\langle v \rangle}; \quad \langle v \rangle = \frac{v_{max,wall} + v_{max,axis}}{2}, \tag{1}$$

where r_x and r_z are the vortex radial and axial radii ($r_r \approx 79mm$, $r_z \approx 142mm$) and $\langle v \rangle$ is the halved sum of maximal velocity near the wall and that on the symmetry axis averaged for both the top and the bottom vortices.

3. The modeling of low-frequency oscillations Large eddies are computed directly and the smallest eddies are modeled in the LES method[4]. The boundary conditions usually affect the largest eddies, while the small-scale turbulence is more isotropic. It was shown that the LES could be successfully used

to model low-frequency velocity oscillations in the recirculating melt flow [3, 5], however this method requires large computer resources.
Large number of elements and LES provide the best modeling results as compared to experimental data [3]. The RNG-based subgrid-scale model computations give the periods that are very close to experimental, but Smagorinsky-Lilly subgrid-scale model gives a more correct intensity of pulsations [5]. It is very difficult to choose among the approaches. The RNG subgrid-scale model was selected for our calculations, because it gives more correct results at low Reynolds numbers and accounts for the near-wall effects. At high Reynolds numbers this reduces to the Smagorinsky-Lilly model with a different model constant [6].
The use of millions of elements in a numerical LES simulation makes it almost impossible to do such calculations on a usual modern PC for the model of real experiment. It is also possible to perform unsteady modeling of recirculated flow using 3D Reynolds averaged Navier-Stokes equations in conjunction with a Reynolds stress turbulence model [7], but the real LES calculations can be done in the way described below.
First, the Lorentz force was computed using a simple axially-symmetric model in the commercial finite element package *ANSYS*. The force is almost symmetric relative to the $y = 0$ plane (figure 10); some asymmetry takes place because of the crucible geometry. We have taken only radial component of the force and approximated it with a fourth power polynomial for the model because the ratio of penetration depth $\delta = \frac{1}{\sqrt{\pi \sigma f \mu_0}}$ to the crucible radius changes from 0.08 at 1500 Hz to 0.18 at 300 Hz.
The model's geometry was simplified to obtain smaller number of elements and to perfom the LES simulation on a laboratory PC (Pentium 4 2.4 GHz with 533 MHz bus and 512 MB DDR memory) in *FLUENT 6.1.22* environment. The model, which was used in *FLUENT*, had a rectangular tank form (figure 11). Its sizes were similar to the experimental ones (height 570 mm,width 316 mm). The depth of the tank (z-direction) was selected 100 mm. The number of elements in the model was about 216000. The grid resolution was about $3 \div 5$ mm depending on the direction. The front, back and upper planes had free surface boundary conditions. For the rest of walls no slip boundary conditions were observed. The *ANSYS* calculated force was applied symmetrically to the left and the right planes of the tank using *FLUENT*'s UDF functions. This force varied for different calculation sets.
For fluent calculations different schemes were used. The $k - \varepsilon$ model was sometimes employed to obtain the initial distribution of velocity field of the flow and to reduce the total time of calculations. Then a transient LES flow simulation was done. Some calculations were performed on a model, where the force was applied to the melt at rest. The time step and their number differed for each simulation and depended on the characteristic velocity of the flow or, in other words, on the period of vortex circulation. Time step values were selected between 0.01 s and 0.05 s, with their total number being about 13500 in some simulations.
For each time step the middle cross-section was defined and the values of velocity components were saved in the profile files. For the correlation and Fourier analysis of the profile files special software was developed.

4. Results of computations The computations were performed on models with different EM forces. A model with a small Lorentz force (16% of the rated, which corresponds to the 1400 A inductor current) was implemented to see how

the flow is developed in time. Nine minutes of the real flow were calculated with the time step of 0.04 s. The characteristic velocities of such flow were below 1 cm/s (with Re about 3400) and the period of vortex circulation was about 40 s, which means that the selected time step was fully appropriate. The maximal number of iterations per time step was set equal to 30 and the total count of time steps was 13500. The melt was in the rest at zero time and the motion of the melt began when force was applied. The velocity values were growing, achieving their maximum after about 70 flow seconds (figure 12). Then the melt flow stabilized and approximately after 240 s low-frequency oscillations began. These calculations were done using first-order upwind approximation for momentum equations. The Fourier analysis was performed for each stage of flow development. The first stage of the flow when the velocities are growing does not contain characteristic frequencies. The spectrum covering the time of flowing from 82 to 245 s contains some low frequencies, which can be explained as instabilities of vortex development (figure 13). This flow is not explicitly turbulent, since Fourier's spectra do not contain high harmonics and the oscillation energy is small. The flow fully develops to turbulent after about 240 s of the run and the spectra of the last stage are typical of turbulent flow containing lots of frequencies. The intensity of such turbulent spectrum is at least one order greater than that in the second stage. This spectrum also has low frequency part, in which the largest part of energy is found.

The flow development is laminar until the Reynolds number reaches values above 2000 (the corresponding velocity is about 0.8 cm/s). Then some instability develops so that z-velocity component, which is not influenced by the Lorentz force, also starts to oscillate. Our numerical approach gives a good qualitative pattern of the flow development.

The following calculations were performed with the force, which is 80% of the rated value. The maximum flow velocity near the wall is about 7.5 cm/s in this case (Re $\sim$25000). The mesh was the same and the stationary $k-\varepsilon$ solution was selected as the initial state for the LES model. No calculations of the rest state were performed since they need a small time-step to obtain solution convergence at high force values. In the present calculations the central difference scheme for momentum equations was applied. The time step was the same and two minutes of the flow were computed (figure 14). The flow pattern at every time step is not symmetric because of the high turbulence, but averaged flow is fully symmetrical. The computed averaged flow shows a zone in the middle of the tank, between vortices in which flow intensity is low. The height of this zone is about 10 cm. The velocity vectors change their values and direction depending on the "strength" of interacting eddies at every time moment. The "strongest" eddy stops transferring its energy to another eddy because of which the process begins again. A typical Fourier's spectrum and the correlation spectrum are shown on figure 15. There are several frequencies in Fourier's spectrum, at which the energy values are large, but correlation analyses gives the basic frequencies of pulsations (for example, the basic frequency of pulsations on figure 15 (right) is about 7 s).

Two series of calculations were made with the rated force corresponding to the 1400 A current. The time step in both calculations was 0.05 s. The only difference was the scheme used for the momentum equations: first-order upwind or central-difference scheme. The calculations were performed in order to check whethers the facts that first-order upwind momentum equations reduce the intensity of pulsations [6]. The FFT analysis for both calculations show that the difference in the spectra at using the first-order upwind and central differences schemes for the momentum equations is about 5-10 times at the region of low frequencies (figure

16). Here again we have several frequencies of equal energies in the spectrum in the model based on the central-difference scheme (figure 16 right).
The smallest frequency we have found was about 0.025 Hz, which gives a period of 40 s. That is why such a long calculation time is needed. This frequency is characteristic of all the models, so it can be defined by the model geometry.
The calculated flow parameters are shown in table 2. The pulsation period is of the same order as the eddy circulation period. More precise comparison is difficult to make since different methods for calculation of averaged velocity can be applied. The calculated averaged velocities are smaller than the equivalent velocities from the experiments because of different model geometry. The maximum flow velocities are in the by-wall region. They are of the same order as the measured averaged velocities at the symmetry axis.

f/f_{nom}	Eddy period, s	Pulsation period, s	$\langle v \rangle$, cm/s (calc)	Discretization	$\langle v \rangle$, cm/s (exp)
0.16	115.0	40	0.6	First order	
0.80	20.9	20	3.3	Centr. dif.	5.92
1.00	13.8	17	5.0	First order	8.36
1.00	14.7	10	4.7	Centr. dif.	8.36

Table 2: Calculated flow parameters

5. Conclusions In the paper preliminary analysis of the turbulent recirculated flow has been performed using simplified models of the flow in a rectangular tank geometry. The calculated results are of the same order as the measured in experiment and are in qualitative agreement with experimental and literature data. More sophisticated models based on the real geometry of the studied process should be used for better quantitative agreement of calculations with experimental data. The low-frequency velocity oscillations have been computed using different momentum discretization schemes. Each approach leads to the pulsations, but calculated flow parameters are different. The model proposed by us makes it possible to work out a qualitative approach to the development of the turbulent flow from the rest state to the state of high turbulence; it also can be used to perform the heat-and-mass transfer analysis of real systems.

Acknowledgements This paper has been supported by the *European Social Fund (ESF).*

REFERENCES

1. V. Bojarevics, R. A. Harding, K. Pericleous, and M. Wickins. The development and experimental validation of a numerical model of an induction skull melting furnace. *Metallurgical and materials transactions B*, vol. 35B (august 2004), pp. 785–803.
2. E. Baake. *Grenzleistungs- und Aufkohlungsverhalten von Induktions-Tiegelöfen* (VDI, Düsseldorf, 1994)
3. A. Umbrashko, E. Baake, B. Nacke and A. Jakovics. Modeling of the turbulent flow in induction furnaces. (to be published).
4. P. Sagaut. *Large Eddy Simulation for Incompressible Flows, 2nd edition* (Springer, 2002)

5. E. Baake, B. Nacke, A. Umbrashko, A. Jakovics. Large eddy simulation modeling of heat and mass transfer in turbulent recirculated flows. *Magnetohydrodynamics*, vol. 39 (2003), no. 3–4.

6. Fluent 6.0 Users's guide, 2001.

7. R. Schwarze and F. Obermeier Modelling of unsteady electromagnetically driven recirculating melt flows *Modelling Simul. Mater. Sci. Eng.*, vol. 12 (2004), pp. 985–993.

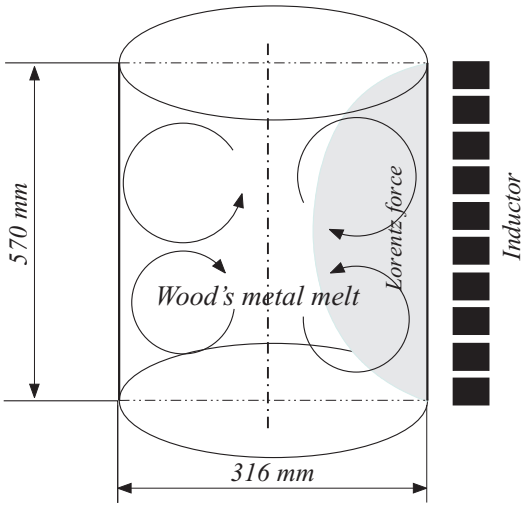

Figure 1: Design of the experimental crucible induction furnace with sketch of typical vortices of mean flow

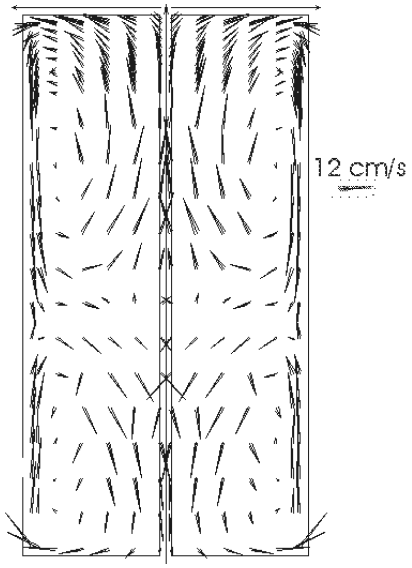

Figure 2: Averaged flow (experimental data, crucible filling level is 110%)

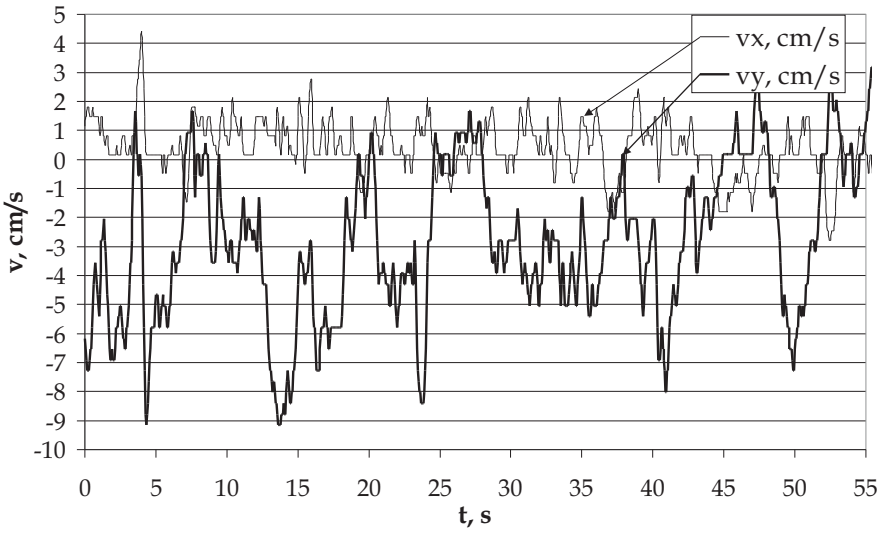

Figure 3: Example of measured velocity (the point selected is near the crucible wall between the vortices)

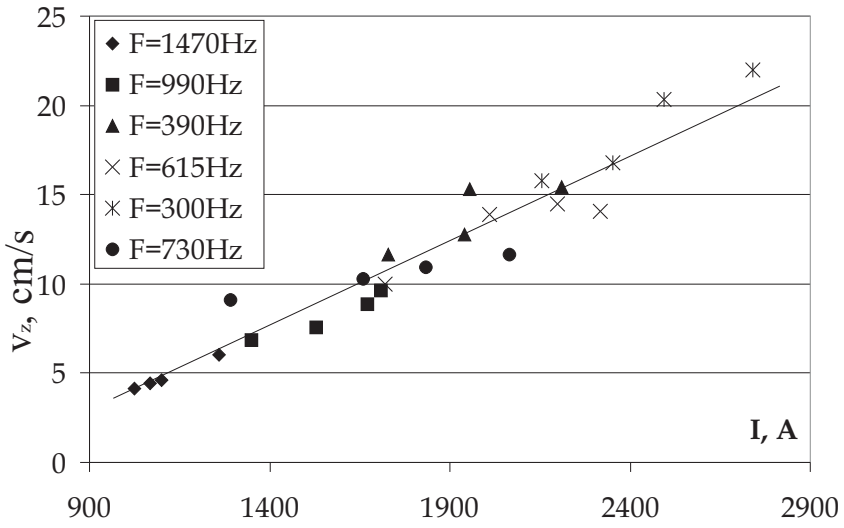

Figure 4: Maximum axial velocity $v_z max$ dependence on the inductor current for different frequencies at the symmetry axis point $r = 0$, $z = 130mm$

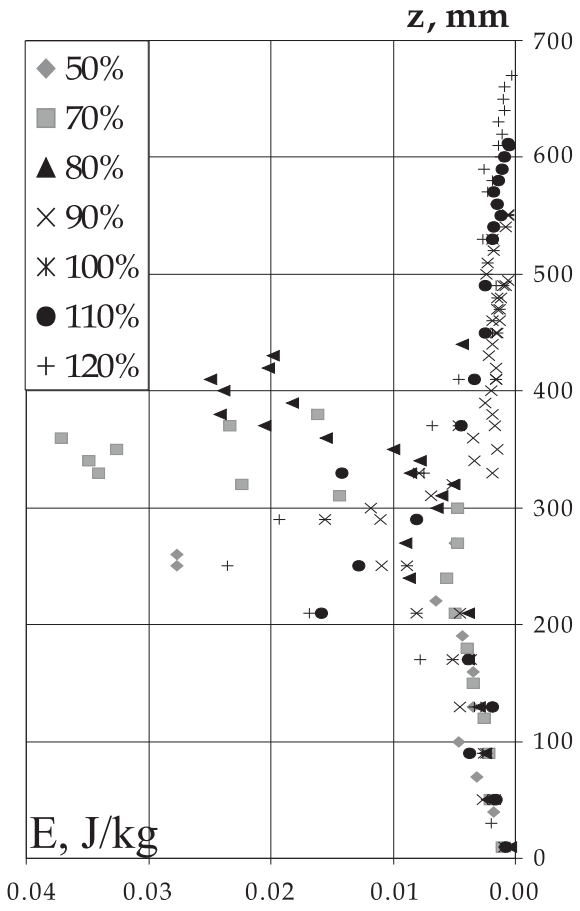

Figure 5: Kinetic energy of pulsations vs. height near the crucible wall for different filling levels

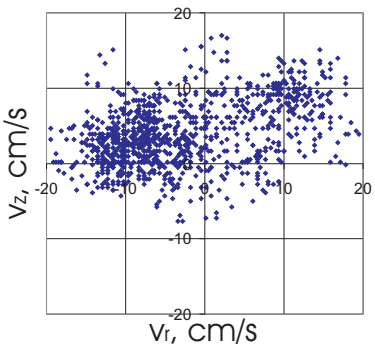

Figure 6: Velocity components, $r = 0, z = 250mm, \langle v_z \rangle = 3.9cm/s$

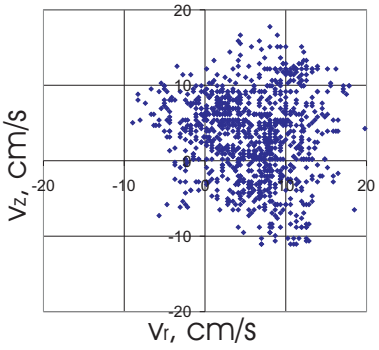

Figure 7: Velocity components, $r = 90mm, z = 250mm, \langle v_r \rangle = 5.7cm/s, \langle v_z \rangle = 3.2cm/s$

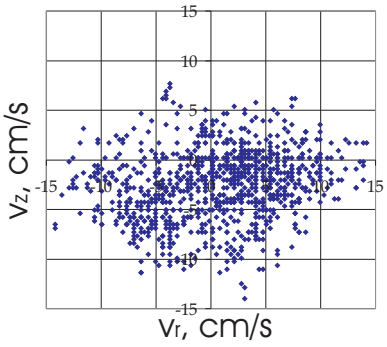

Figure 8: Velocity components, $r = 0, z$ is between eddies, $\langle v_r \rangle = 0.9cm/s, \langle v_z \rangle = -2.5cm/s$

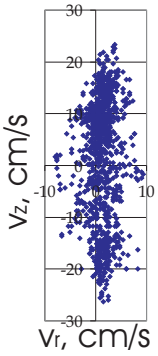

Figure 9: Velocity components, $r = 147mm, z$ is between eddies, $\langle v_r \rangle = 1.2cm/s, \langle v_z \rangle = 1.7cm/s$

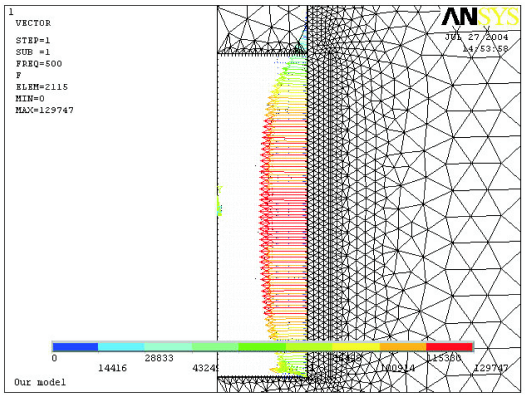

Figure 10: *ANSYS* calculated Lorentz force

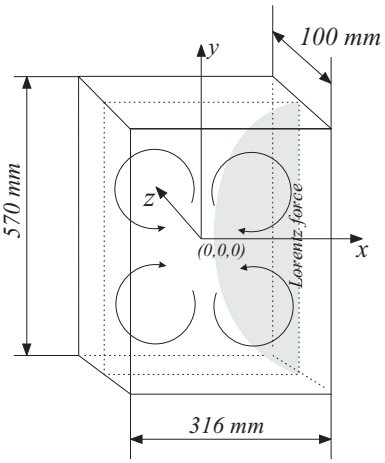

Figure 11: Design of the model

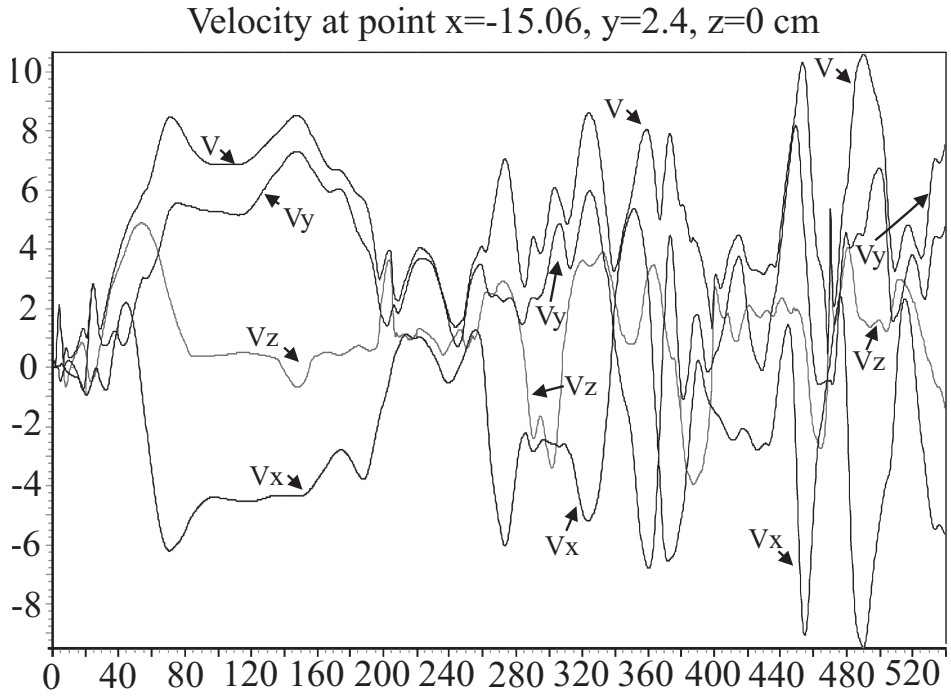

Figure 12: Time dependence of the flow velocity between eddies near the wall for small Lorentz force (16% of rated)

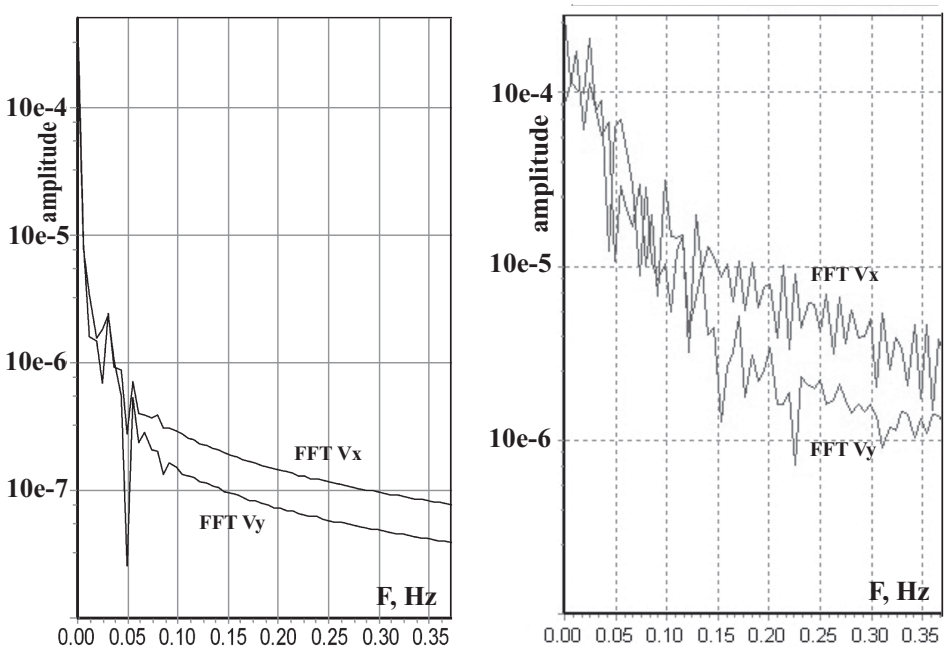

Figure 13: FFT velocity at the begining of the flow (80-240 s, left) and in the fully developed flow (right), force is 16% of rated

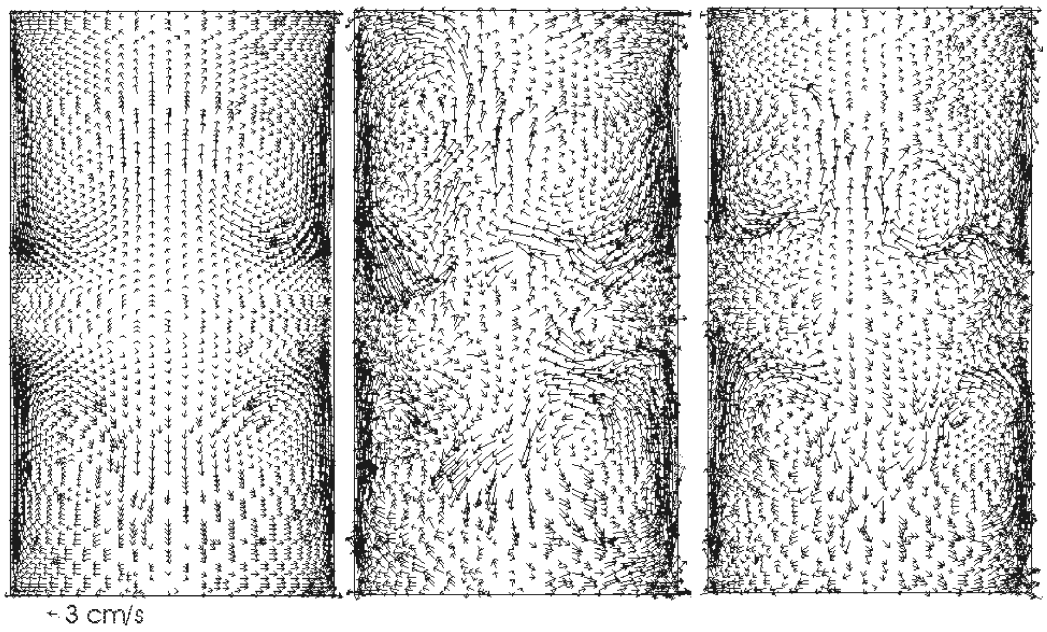

Figure 14: Flow pattern in the middle plane (averaged, at 20, 100 s. Force is rated and corresponds to current 1400 A)

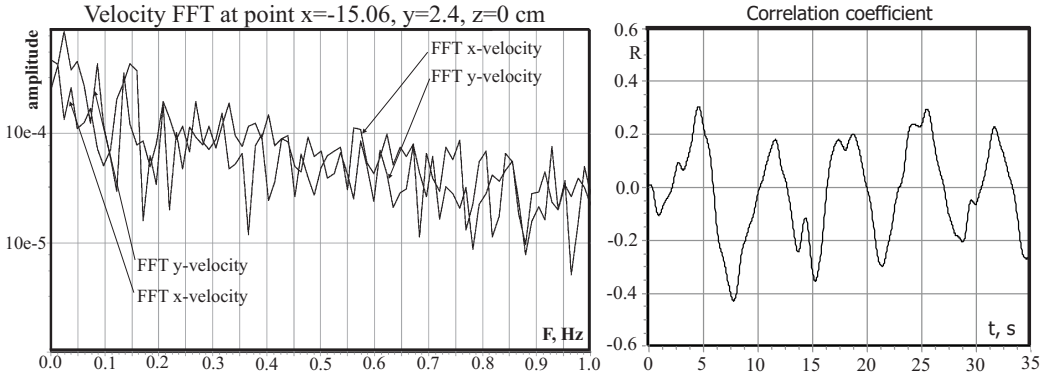

Figure 15: FFT velocity and correlation spectra at the point near the wall between vortices. Force is 80% of rated (central differences discretization)

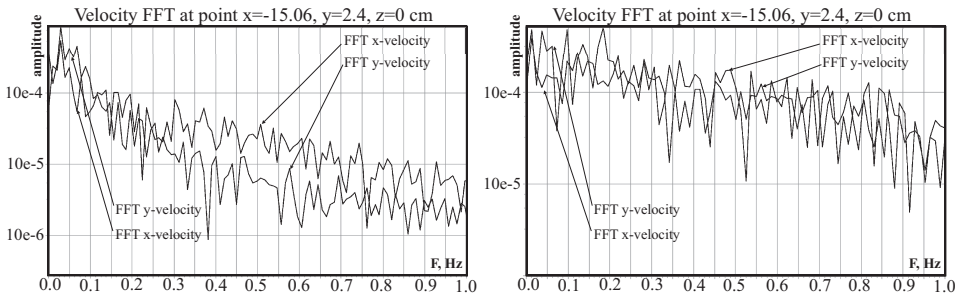

Figure 16: FFT velocity corresponds to calculations performed with the first-order (left) and with the central-difference scheme (right) for the momentum equations